LETTER

doi:10.1038/nature11202

Magnetic tornadoes as energy channels into the solar corona

Sven Wedemeyer-Böhm[1,2], Eamon Scullion[1], Oskar Steiner[3], Luc Rouppe van der Voort[1], Jaime de la Cruz Rodriguez[4], Viktor Fedun[5] & Robert Erdélyi[5]

Heating the outer layers of the magnetically quiet solar atmosphere to more than one million kelvin and accelerating the solar wind requires an energy flux of approximately 100 to 300 watts per square metre[1–6], but how this energy is transferred and dissipated there is a puzzle and several alternative solutions have been proposed. Braiding and twisting of magnetic field structures, which is caused by the convective flows at the solar surface, was suggested as an efficient mechanism for atmospheric heating[7]. Convectively driven vortex flows that harbour magnetic fields are observed[8–10] to be abundant in the photosphere (the visible surface of the Sun). Recently, corresponding swirling motions have been discovered[11] in the chromosphere, the atmospheric layer sandwiched between the photosphere and the corona. Here we report the imprints of these chromospheric swirls in the transition region and low corona, and identify them as observational signatures of rapidly rotating magnetic structures. These ubiquitous structures, which resemble super-tornadoes under solar conditions, reach from the convection zone into the upper solar atmosphere and provide an alternative mechanism for channelling energy from the lower into the upper solar atmosphere.

Chromospheric swirls are seen as narrow rotating rings (or ring fragments) in the core of the singly ionized calcium (Ca II) 854.2-nm absorption line that is formed in the chromosphere (Fig. 1b–d). Their diameters are typically of the order of 1,500 km, which is thousands of times larger than the diameters of terrestrial tornadoes. Swirls appear dark in the spectral line core images and have Doppler shifts corresponding to upward (line-of-sight) velocities of typically 4 km s^{-1}, with even larger peak values (Fig. 1d, Dopplergram). We detect a corresponding response in the atmospheric layers above the chromosphere by using the 30.4-nm (He II), 17.1-nm (Fe IX), 19.3-nm (Fe XII and Fe XXIV) and 21.1-nm (Fe XIV) channels of the SDO/AIA[12] (Figs 1d and 2c). We found 14 swirls with an average lifetime of 12.7 ± 4.0 min during a 55-min-long observation sequence on 8 May 2011 (Fig. 2a and Supplementary Table 1). Statistically, there were 3.8 swirls in each 1′ × 1′ field at all times, resulting in there always being approximately 1.1×10^4 swirls on the solar surface (Fig. 1a). In view of the observational limitations, this number must be understood as a lower limit.

An exemplary swirl is illustrated in Fig. 1c, d. The chosen wavelength channels of CRISP and AIA effectively map the atmospheric layers with increasing height. The fact that we find a signal at the same

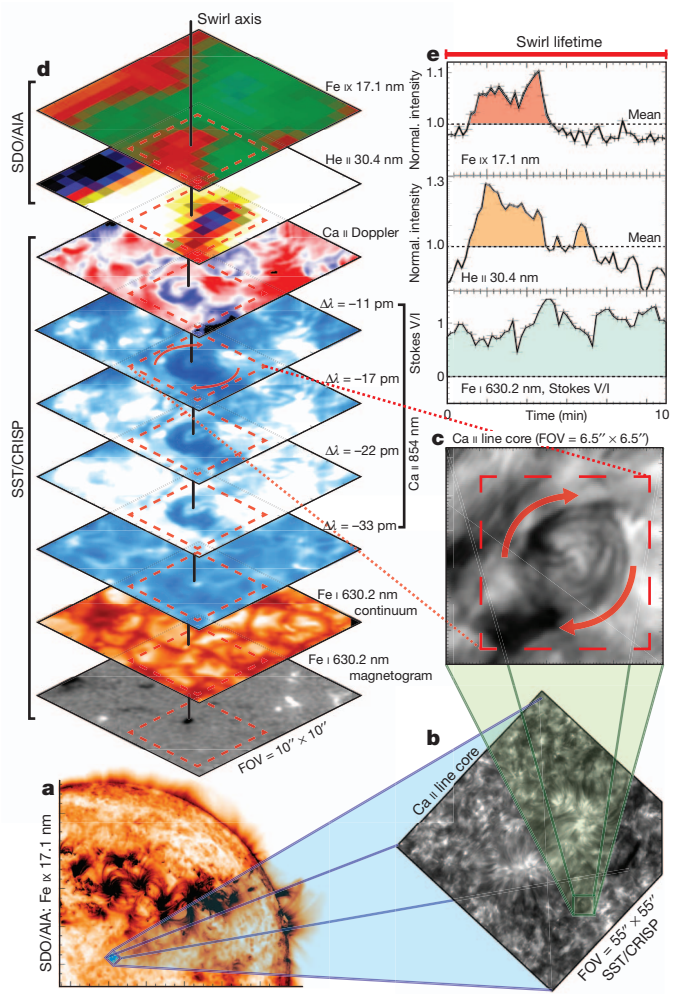

Figure 1 | Observation of a swirl event and its coronal counterpart. Co-aligned and co-temporal solar observations made on 8 May 2011 using the Atmospheric Imaging Assembly (AIA) on board NASA's space-based Solar Dynamics Observatory (SDO) (cadence, 12 s; image scale, 0.6″ per pixel) and the Crisp Imaging Spectropolarimeter (CRISP) on the ground-based, Swedish 1-m Solar Telescope (cadence, 14 s; 47 line positions across the Ca II 854.2-nm spectral line of the infrared triplet; image scale, 0.06″ per pixel). **a**, Part of the full-disk AIA Fe IX 17.1-nm channel with the field of view (FOV) of CRISP at the centre of the solar disk (blue box, 55″ × 55″). **b**, Corresponding CRISP image in the Ca II 854.2-nm line core. **c**, Close-up of the region with a chromospheric swirl. **d**, Layered atmosphere from the photosphere (bottom panel: magnetogram, Fe I 630.2-nm continuum), through the chromosphere (Dopplergram, Ca II 854.2 nm) and the transition region (He II 30.4 nm) to the low corona (top: Fe IX 17.1 nm). The visible radiation of the lower solar atmosphere is compared with high-resolution imaging of the extreme-ultraviolet radiation components. Here it is revealed that tornado-like swirls (**c**), previously only observed in the chromosphere, have a signal in the spectral lines formed in the hot solar corona (**e**). The line-of-sight component of the magnetic field (**e**, bottom) reveals the unipolar nature of the rotating structure. The concurrent transition region (**e**, middle) and low normalized coronal intensity (**e**, top) reveal radiative emission during the lifetime of the swirl, thus implying heating. See Supplementary Movie 1.

[1]Institute of Theoretical Astrophysics, University of Oslo, PO Box 1029 Blindern, N-0315 Oslo, Norway. [2]Center of Mathematics for Applications, University of Oslo, PO Box 1053 Blindern, N-0316 Oslo, Norway. [3]Kiepenheuer Institute for Solar Physics, Schöneckstrasse 6–7, D-79104 Freiburg, Germany. [4]Department of Physics and Astronomy, Uppsala University, Box 516, SE-75120 Uppsala, Sweden. [5]Solar Physics and Space Plasma Research Centre, School of Mathematics and Statistics, University of Sheffield, Hicks Building, Hounsfield Road, Sheffield S3 7RH, UK.

location in each subsequent co-aligned layer implies that these layers are connected by a coherent structure (visualized by the swirl axis in Fig. 1d). The enhanced normalized intensities in the 30.4-nm and 17.1-nm channels, integrated across the swirl region (Fig. 1d, dashed boxes), shows that this event channels energy into the transition region and low corona (Fig. 1e). A signal in the 30.4-nm channel is found for all 14 swirls. Four of them also show co-aligned emission in the AIA channels at 19.3 and 21.1 nm, which implies that the vertical extents of the individual swirls vary (Fig. 2b and Supplementary Table 1).

We found that at exactly the same spatial position as each swirl, there is at least one or often several bright points in the corresponding Fe I continuum intensity, which maps the photospheric surface (Fig. 1d). These bright points are the observational signature of the footpoints of magnetic flux concentrations as seen in the simultaneously recorded magnetogram (Fig. 1d). The time series of the magnetograms (Fig. 1e, bottom) shows that the magnetic polarity and total magnetic flux are conserved during the lifetime of the swirls, which makes it unlikely that magnetic reconnection occurred. The observations also strongly suggest that swirls are connected to magnetic field structures that couple the layers of the solar atmosphere from the photosphere to the corona. This conclusion is further supported by the fact that the cross-section of the swirl feature increases with height, which is a fundamental property of expanding magnetic structures[13].

The solar surface is characterized by horizontally divergent flow fields in the bright granular plasma updrafts, which converge into the dark network of intergranular lanes. There the cooled plasma sinks down again into the solar interior. In particular, at the vertices of the lanes the conservation of angular momentum of an initially weak, net angular motion of the inflowing plasma results in the formation of vortex flows. This 'bathtub effect'[14] is observed in a wide variety of hydrodynamical systems, for example in tornadoes in Earth's atmosphere[15]. The predicted vortex flows are commonly observed in the

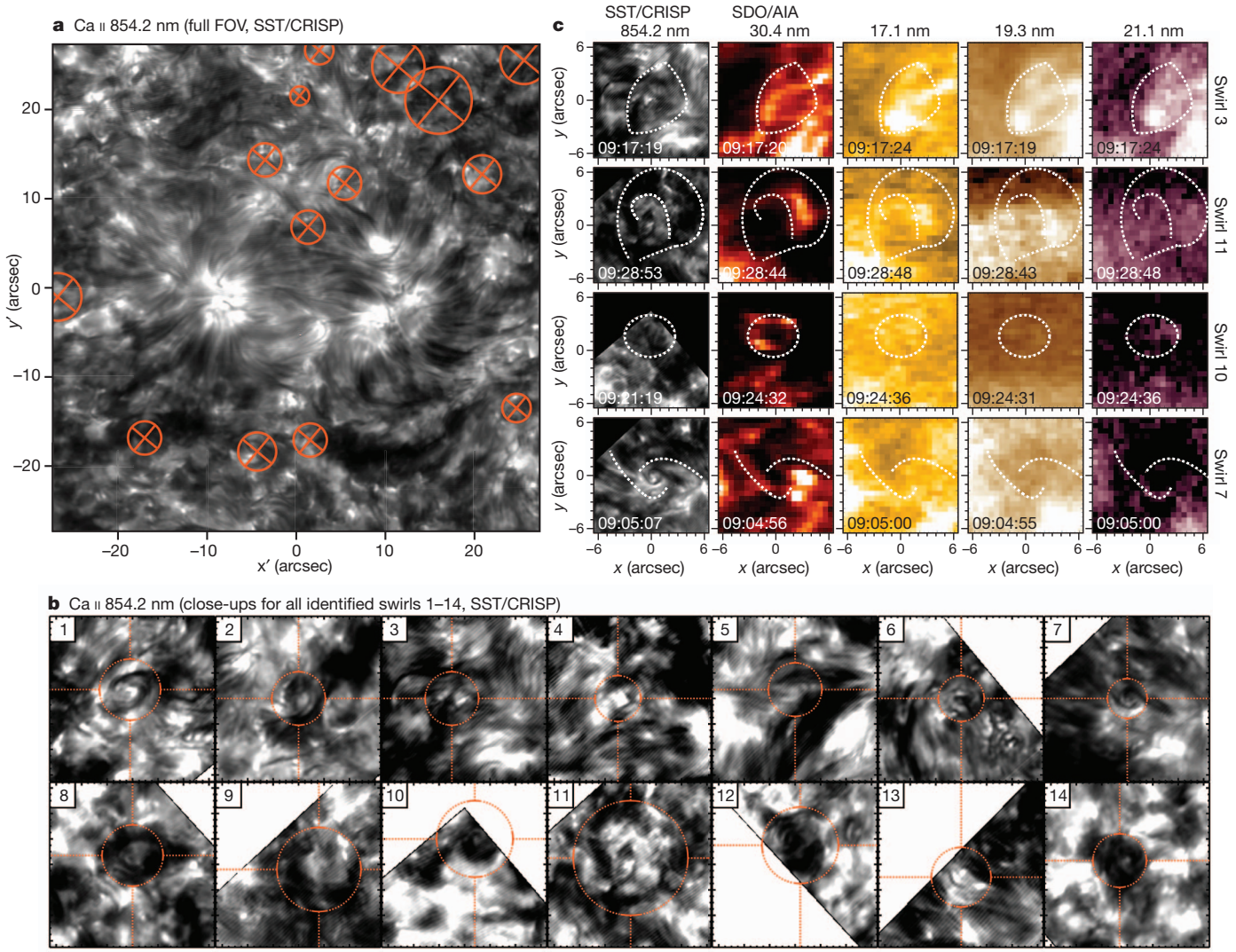

Figure 2 | Detected swirl events in the solar observations on 8 May 2011. **a**, Field of view of SST/CRISP at the centre of the solar disk (spatial coordinates x' and y' refer to the de-rotated image), with all identified swirls marked with crosses and circles on top of an exemplary image in the Ca II 854.2-nm spectral line core. The size of the circles represents the area attributed to the individual swirls. **b**, Close-ups (field of view 13″ × 13″) of the Ca II 854.2-nm line core maps for each of the 14 swirls (Supplementary Movie 2). **c**, Comparison of the Ca II images, and the SDO/AIA channels at 30.4, 17.1, 19.3 and 22.2 nm for four selected examples labelled on right. Swirl 3 is the hottest event with the strongest emission in the swirl centre in the 21.1-nm channel. There is also strong emission in the swirl ring fragments in all SDO/AIA channels. Swirl 11 is the largest in terms of spatial area, and the swirl arc (outlined with white contours in the Ca II map) contains hot components in all SDO channels. The hottest (21.1-nm) signal is sourced to the leading edge of the front of the swirl arc. Swirl 10 reveals a distinct ring formation in the 30.4-nm SDO channel and weaker signal in the other SDO maps. We detect a propagating signal in the ring formed in the 30.4-nm SDO channel, which occurs in unison with the swirl arc in the Ca II map. Likewise, with swirl 7 we observe the swirl structure in the ring in all four SDO channels. Swirl 1 is shown in more detail in Fig. 1. See Supplementary Table 1.

solar photosphere on various spatial scales ranging from over several thousand kilometres[8] down to 1,000 km and smaller[9,10]. Photospheric vortex flows have also been found in high-resolution numerical simulations of the solar atmosphere[16–20], including those presented here. Despite the apparent similarities between previously observed photospheric vortex flows[8,9] and chromospheric swirls, the formation of chromospheric swirls is most likely related to the convective motions on even smaller spatial scales.

We validate this hypothesis with a detailed analysis of simulations carried out with the three-dimensional, radiative magnetohydrodynamics codes CO^{5}BOLD[21] (Fig. 3) and BIFROST[22] (Supplementary Fig. 1). The generated granular flows reorganize the magnetic field, which is essentially advected passively under the conditions of the low photosphere in quiet Sun regions. The result of this reorganization is a complex magnetic field topology where footpoints are concentrated in the intergranular downflow lanes in the form of knots and sheets (Fig. 3a, e). This process generates high magnetic field strengths, in excess of 0.1 T, in the lane vertices where the vortex flows are found. It has been observed directly that such small-scale magnetic concentrations are continuously dragged by vortex motions[23,24]. Consequently, the bathtub effect causes the footpoints of magnetic field structures to rotate.

The magnetic field itself effectively couples the different layers of the solar atmosphere and transfers the rotation of the footpoints into the upper layers (Fig. 1d). Whereas the magnetic footpoints are forced to follow the photospheric flow field, the situation is reversed in the layers above. There the magnetic pressure dominates over the gas pressure, such that the plasma motion is forced to follow the magnetic field. This process, which is probably also responsible for the 'solar cyclones' observed on larger spatial scales[25], is characteristic in our numerical simulations. A close-up of an exemplary region with a chromospheric swirl is shown in Fig. 3. The magnetic field lines (Fig. 3a, b, red lines) are concentrated in the photospheric footpoints (Fig. 3e) and expand in the atmosphere above, where the field stays largely vertically aligned.

Driven by the overshoot of granular flows into the photosphere and by the omnipresent 5-min oscillations at the solar surface, gas moves up and down throughout the photosphere and the chromosphere. At the location of a swirl, the matter following the rotating field lines is effectively forced into spiral trajectories (Fig. 3a, b, blue–green lines) as the field expands with height. This small-scale, tornado-like vortex structure is easily detected as a ring of increased horizontal velocity at chromospheric heights (Fig. 3c) and also as confined regions of enhanced vorticity (Fig. 3d). The diameter of the rotating flux structure increases with height in the atmosphere, owing to the decrease in the gas pressure that balances the magnetic pressure in the structure. The structure is thus much narrower in the photosphere than in the less dense chromosphere and rotates approximately as a rigid body (Fig. 3f).

The simulations provide a realistic description of the solar atmosphere, which is validated by a detailed comparison of corresponding synthetic intensity maps with the observations (Supplementary Fig. 2). The excellent agreement regarding the pattern in the line core maps and also the Doppler shifts confirms that chromospheric swirls are indeed the observational tracers of rotating magnetic flux structures. The analysed CO^{5}BOLD model contains 11 additional smaller examples. A similar swirl signature is found in numerical simulations with BIFROST (Supplementary Fig. 1).

The fast rotation of the magnetic flux structures generates a centrifugal force that moves the contained plasma outwards along the slanted magnetic field lines (Fig. 3a, b). The rotation axis of the swirl, and with it the whole structure, is tilted and twisted and changes with height and time. The axis of the example shown in Fig. 3 is inclined with respect to

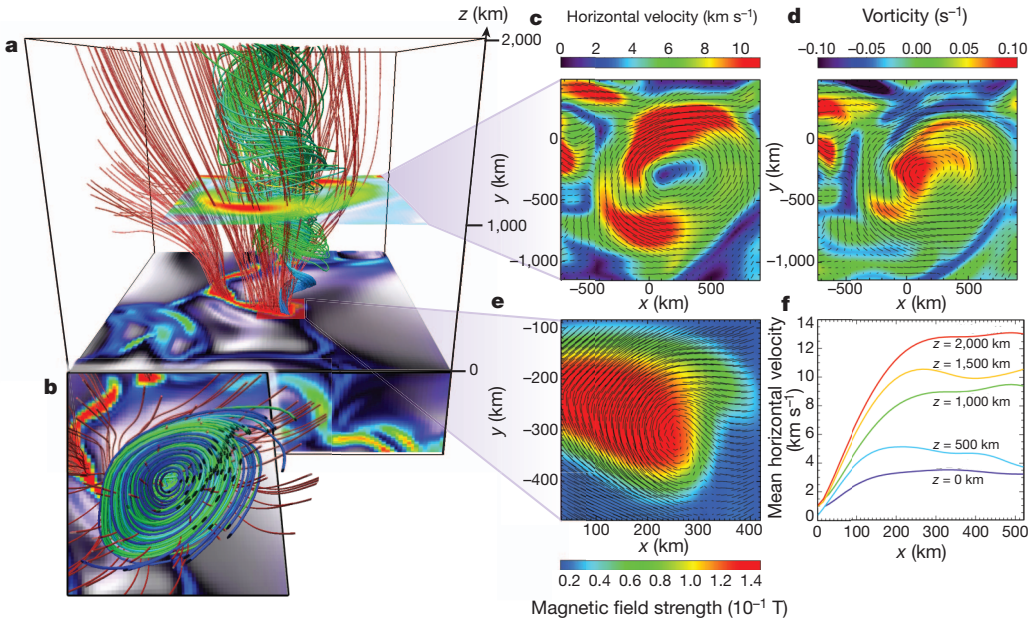

Figure 3 | Numerical model of a swirl event produced with CO^{5}BOLD. **a**–**e**, The displayed close-up region (**a**) is part of the evolved model, which has an overall horizontal size of 8,000 km × 8,000 km and extends vertically from 2,400 km below the surface to the top of the chromosphere at an altitude of 2,000 km. The initial magnetic field was vertical and homogeneous, with a field strength of 5 mT. Periodic lateral boundary conditions and an open lower boundary condition were used, whereas the top boundary has transmitting hydrodynamic and radiative boundary conditions. The three-dimensional geometry of the region around the swirl is visualized with VAPOR[30] from the side (**a**) and from the top (**b**). Next to the (photospheric) surface at $z = 0$ km (grey plane with granulation pattern and overlaid magnetic field strength), the magnetic field lines are plotted as red lines. The plasma flows along and co-rotates with the magnetic field, resulting in spiral trajectories (blue–green streamlines following the velocity field). The swirl is clearly seen in the horizontal velocity (**c**) and the vorticity (**d**) in horizontal cross-sections at a height of $z = 1{,}000$ km (middle chromosphere). The arrows map the horizontal flow field. The bathtub effect is clearly visible in the close-up (**e**) of the magnetic footpoint in the intergranular lane ($z = 0$ km). The resulting rotation is mediated to the chromosphere above by the magnetic field, which effectively couples the atmospheric layers. It produces a rotating funnel in the chromosphere. The corresponding radial velocity profiles (**f**) show that the structures undergo quasi-rigid-body rotation within a cut-off radius, which increases with height. See Supplementary Movie 3.

the vertical by an angle mostly between 10° and 20°. Gas parcels can thus be effectively accelerated upwards in the inclined flux structure, against gravity. The observations indeed show the greatest upward velocity to be in the outer, ring-like regions of swirls, where the centrifugal forces are strongest (Supplementary Fig. 2d, h).

Furthermore, torsional Alfvén waves[26,27] that are generated by the vortex flow in the photosphere and chromosphere propagate upwards and direct part of the associated Poynting flux vertically[28]. The analysed swirl has a net Poynting flux component parallel to the swirl axis that amounts to $1.4 \times 10^4\,\mathrm{W\,m^{-2}}$ measured over the effective swirl area at the top of the model (Supplementary Fig. 3). We estimate a net positive Poynting flux of $440\,\mathrm{W\,m^{-2}}$ averaged over the computational box (Supplementary Notes). This energy flux is delivered at the transition region and, thus, at the boundary to the low corona, where it could be transformed into a substantial heating contribution and emission of radiation, accounting for the signals that we observed with SDO/AIA (Figs 1d and 2c). There the related Alfvén waves generate current sheets when interacting with pre-existing magnetic fields, or potentially cascade to the high-frequency waves[29] needed to drive the fast solar wind from coronal holes. The discovery of this process demonstrates that the energy that reaches the transition region is generated by vortex driving of the magnetic footpoints on small spatial scales at the top of the convection zone, and is then channelled into the outer solar atmosphere by magnetic fields.

Received 7 February; accepted 24 April 2012.

1. Parker, E. Dynamical theory of the solar wind. *Space Sci. Rev.* **4,** 666–708 (1965).
2. Priest, E. *et al.* Nature of the heating mechanism for the diffuse solar corona. *Nature* **393,** 545–547 (1998).
3. Schrijver, C. *et al.* Large-scale coronal heating by the small-scale magnetic field of the Sun. *Nature* **394,** 152–154 (1998).
4. De Pontieu, B. *et al.* Chromospheric Alfvénic waves strong enough to power the solar wind. *Science* **318,** 1574–1577 (2007).
5. Cirtain, J. *et al.* Evidence for Alfvén waves in solar X-ray jets. *Science* **318,** 1580–1582 (2007).
6. McIntosh, S. *et al.* Alfvénic waves with sufficient energy to power the quiet solar corona and fast solar wind. *Nature* **475,** 477–480 (2011).
7. Parker, E. Nanoflares and the solar X-ray corona. *Astrophys. J.* **330,** 474–479 (1988).
8. Brandt, P., Scharmer, G., Ferguson, S., Shine, R. & Tarbell, T. Vortex flow in the solar photosphere. *Nature* **335,** 238–240 (1988).
9. Bonet, J., Márquez, I., Sánchez Almeida, J., Cabello, I. & Domingo, V. Convectively driven vortex flows in the Sun. *Astrophys. J.* **687,** L131–L134 (2008).
10. Bonet, J. *et al.* SUNRISE/IMaX observations of convectively driven vortex flows in the Sun. *Astrophys. J.* **723,** L139–L143 (2010).
11. Wedemeyer-Böhm, S. & Rouppe van der Voort, L. Small-scale swirl events in the quiet Sun chromosphere. *Astron. Astrophys.* **507,** L9–L12 (2009).
12. Lemen, J. *et al.* The Atmospheric Imaging Assembly (AIA) on the Solar Dynamics Observatory (SDO). *Sol. Phys.* **275,** 17–40 (2012).
13. Tu, C.-Y. *et al.* Solar wind origin in coronal funnels. *Science* **308,** 519–523 (2005).
14. Nordlund, Å. Solar convection. *Sol. Phys.* **100,** 209–235 (1985).
15. Bøhling, L., Andersen, A. & Fabre, D. Structure of a steady drain-hole vortex in a viscous fluid. *J. Fluid Mech.* **656,** 177–188 (2010).
16. Stein, R. & Nordlund, Å. Simulations of solar granulation. I. General properties. *Astrophys. J.* **499,** 914–933 (1998).
17. Steiner, O. *et al.* Detection of vortex tubes in solar granulation from observations with SUNRISE. *Astrophys. J.* **723,** L180–L184 (2010).
18. Shelyag, S., Keys, P., Mathioudakis, M. & Keenan, F. Vorticity in the solar photosphere. *Astron. Astrophys.* **526,** A5 (2011).
19. Moll, R., Cameron, R. & Schüssler, M. Vortices in simulations of solar surface convection. *Astron. Astrophys.* **533,** A126 (2011).
20. Kitiashvili, I., Kosovichev, A., Mansour, N. & Wray, A. Excitation of acoustic waves by vortices in the quiet Sun. *Astrophys. J.* **727** L50, (2011).
21. Freytag, B. *et al.* Simulations of stellar convection with CO^{5}BOLD. *J. Comput. Phys.* **231,** 919–959 (2012).
22. Gudiksen, B. *et al.* The stellar atmosphere simulation code Bifrost. Code description and validation. *Astron. Astrophys.* **531,** A154 (2011).
23. Balmaceda, L., Vargas Domínguez, S., Palacios, J., Cabello, I. & Domingo, V. Evidence of small-scale magnetic concentrations dragged by vortex motion of solar photospheric plasma. *Astron. Astrophys.* **513,** L6 (2010).
24. Attie, R., Innes, D. & Potts, H. Evidence of photospheric vortex flows at supergranular junctions observed by FG/SOT (Hinode). *Astron. Astrophys.* **493,** L13–L16 (2009).
25. Zhang, J. & Liu, Y. Ubiquitous rotating network magnetic fields and extreme-ultraviolet cyclones in the quiet Sun. *Astrophys. J.* **741,** L7 (2011).
26. Jess, D. *et al.* Alfvén waves in the lower solar atmosphere. *Science* **323,** 1582–1585 (2009).
27. Fedun, V., Shelyag, S., Verth, G., Mathioudakis, M. & Erdélyi, R. MHD waves generated by high-frequency photospheric vortex motions. *Ann. Geophys.* **29,** 1029–1035 (2011).
28. van Ballegooijen, A., Asgari-Targhi, M., Cranmer, S. & DeLuca, E. Heating of the solar chromosphere and corona by Alfvén wave turbulence. *Astrophys. J.* **736,** 3 (2011).
29. Cranmer, S., van Ballegooijen, A. & Edgar, R. Self-consistent coronal heating and solar wind acceleration from anisotropic magnetohydrodynamic turbulence. *Astrophys. J.* **171** (suppl.), 520–551 (2007).
30. Clyne, J., Mininni, P., Norton, A. & Rast, M. Interactive desktop analysis of high resolution simulations: application to turbulent plume dynamics and current sheet formation. *N. J. Phys.* **9,** 301 (2007).

Supplementary Information is linked to the online version of the paper at www.nature.com/nature.

Acknowledgements We acknowledge discussions with R. Hammer, M. Carlsson, V. Hansteen and S. McIntosh. M. Carlsson and B. Gudiksen are thanked for providing BIFROST simulation data and input on its analysis. This work was supported by the Research Council of Norway including computing time through the Programme for Supercomputing (Notur). R.E. acknowledges M. Kéray for encouragement and is also grateful to the NSF, Hungary. R.E. and V.F. also acknowledge the support received from the Science and Technology Facilities, UK. The Swedish 1-m Solar Telescope is operated on the island of La Palma by the Institute for Solar Physics of the Royal Swedish Academy of Sciences in the Spanish Observatorio del Roque de los Muchachos of the Instituto de Astrofísica de Canarias. We thank the Computational Information Systems Laboratory at the National Center for Atmospheric Research for providing the VAPOR analysis tool.

Author Contributions S.W.-B. and E.S. produced and analysed the data with help from all authors. O.S., V.F. and R.E. gave advice on the data analysis, aspects of the physical interpretation and the applied numerical methods. J.d.l.C.R. and L.R.v.d.V. contributed to the collection and preparation of the observational data and its comparison with numerical data. All authors discussed the results and contributed to and commented on the manuscript.

Author Information Reprints and permissions information is available at www.nature.com/reprints. The authors declare no competing financial interests. Readers are welcome to comment on the online version of this article at www.nature.com/nature. Correspondence and requests for materials should be addressed to S.W.-B. (svenwe@astro.uio.no).